Induction of mitochondrial biogenesis and respiration is associated with mTOR regulation in hepatocytes of rats treated with the pan-PPAR activator tetradecylthioacetic acid (TTA).

Hanne R. Hagland[a], Linn I.H. Nilsson[a], Lena Burri[b], Julie Nikolaisen[a], Rolf K. Berge[b,c], Karl J. Tronstad[a,*]

[a] Department of Biomedicine, University of Bergen, Norway

[b] Institute of Medicine, University of Bergen, Haukeland University Hospital, Norway

[c] Department of Heart Disease, Haukeland University Hospital, Norway

* Corresponding author.

Karl Johan Tronstad,

Department of Biomedicine, University of Bergen

Jonas Lies vei 91, N-5009 Bergen, Norway

Tel: +47 55586433, Fax: +47 55586360, Email: karl.tronstad@biomed.uib.no

Word count: 4587

ABSTRACT

The hypolipidemic effect of peroxisome proliferator-activated receptor (PPAR) activators has been explained by increasing mitochondrial fatty acid oxidation, as observed in livers of rats treated with the pan-PPAR activator tetradecylthioacetic acid (TTA). PPAR-activation does, however, not fully explain the metabolic adaptations observed in hepatocytes after treatment with TTA. We therefore characterized the mitochondrial effects, and linked this to signalling by the metabolic sensor, the mammalian target of rapamycin (mTOR). In hepatocytes isolated from TTA-treated rats, the changes in cellular content and morphology were consistent with hypertrophy. This was associated with induction of multiple mitochondrial biomarkers, including mitochondrial DNA, citrate synthase and mRNAs of mitochondrial proteins. Transcription analysis further confirmed activation of PPARα-associated genes, in addition to genes related to mitochondrial biogenesis and function. Analysis of mitochondrial respiration revealed that the capacity of both electron transport and oxidative phosphorylation were increased. These effects coincided with activation of the stress related factor, ERK1/2, and mTOR. The protein level and phosphorylation of the downstream mTOR targets eIF4G and 4E-BP1 were induced. In summary, TTA increases hepatocyte respiration by inducing hypertrophy and mitochondrial biogenesis in rat, via adaptive regulation of PPARs as well as mTOR.

Key words:

rat hepatocytes; mitochondrial biogenesis; mitochondrial respiration; PPAR; mTOR; hypertrophy

1. Introduction

Metabolic adaptation is linked to life span regulation [1] and important diseases, such as cancer [2], neurodegeneration [3] and obesity-related disorders [4]. Accordingly, mechanisms of metabolic adaptation represent potential targets for prevention and treatment of disease.

The peroxisome proliferator-activated receptors (PPARs) [5,6] and the mammalian target of rapamycin (mTOR) [7,8] are major regulators of metabolism. They converge on the cell survival-associated protein kinase AKT [9], which is involved in insulin signalling and metabolic balancing. The PPARs crosstalk with central metabolic sensors, such as AMP-dependent protein kinase (AMPK) activated upon low energy stress, and PPARγ co-activator 1α (PGC1α) involved in mitochondrial biogenesis, to control adaptive responses [5,6]. The mTOR protein exists in two complexes, named mTOR complex 1/2 (mTORC1/2), where mTORC1 is the primary nutrient responder [8]. Upon activation, mTORC1 promotes protein translation and cell growth via regulation of the downstream eukaryotic translation initiation factor 4E (eIF4E) and the eIF4E-binding protein 1 (4E-BP1) [10]. Upstream regulators of mTORC1 includes AKT [11], AMPK [12] and MAP-kinase-extracellular regulated kinase (ERK) [13].

Metabolic signalling is closely associated with regulation of mitochondrial function and biogenesis. Mitochondria are essential organelles in cellular energy metabolism, and house several catabolic pathways, including fatty acid oxidation, TCA-cycle and mitochondrial respiration. In mitochondrial respiration, electron transport by the respiratory protein complexes is coupled to oxidative phosphorylation yielding ATP from ADP. Regulation of mitochondrial metabolism and respiration is a crucial mechanism of cellular adaptation, e.g. in response to nutritional alterations or energy depletion. For instance, induction of mitochondrial biogenesis can be observed in muscle as a reaction to physical

exercise [14] or mitochondrial mutations [15], and is linked to the actions of AMPK, PPARs and PGC1α. [16]. Multiple important functions of mitochondrial regulators have previously been characterised in rat liver after nutritional and pharmacological interventions [17].

Tetradecylthioacetic acid (TTA) is a modified fatty acid that has hypolipidemic effects in rats [18,19]. This agent activates all the PPAR members, in the ranking order PPARα > PPARδ > PPARγ [19]. Treatment with TTA dramatically increases the mitochondrial oxidative capacity in rat hepatocytes, which seems only partly to be explained by PPAR-activation [17,20]. Here, we used TTA-treatment to investigate the impact and mechanisms of mitochondrial adaptation in relation to key signalling pathways involved in metabolic regulation in rat hepatocytes.

2. Materials and methods

2.1. Materials

TTA was synthesised as described previously [21]. The mtHSP70 and β-actin antibodies were from Abcam (Cambridge, UK), whereas the antibodies for Akt, p-Akt (S473), mTOR 4E-BP1, p-4E-BP1, eIF4G, p-eIF4G, ERK and p-ERK were all from Cell Signaling Technology Inc (Danvers, MA, USA).

2.2. Animals and treatments

The animal study was conducted according to the guidelines for the care and use of experimental animals, and the protocol was approved by the Norwegian State Board of Biological Experiments with Living Animals. Eight to ten week old (150-200g) male Wistar rats were obtained from Taconic Europe (Ry, Denmark) and acclimatised for one week prior to experiment. Control groups were given a normal chow diet, while the TTA-treated group were given chow pellets sprayed with 0.3% (w/w) TTA; both groups were fed ad libitum. The

daily intake of TTA was estimated to 60 mg based on a consumption of 20 g of feed each day. For each experiment, two animals in each group were sacrificed, one for collection of biopsies and one for liver perfusion. Hepatocytes were isolated using in vitro collagenase perfusion as previously described [22,23].

2.3. Transmission electron microscopy (TEM)

Cells and tissue biopsies were fixed in cold 0.1M Na-Cacodylate buffer, pH 7.4, containing 2.5% glutaraldehyde for 15 min. Samples were rinsed with 0.1M Na-Cacodylate buffer for 10 min and post-fixed in 1% osmium tetraoxide (OsO4) for 60 min. Following ethanol dehydration, the samples were embedded in epoxy resin. Ultra-thin sections were prepared and double-stained with uranyl acetate and lead citrate. Microscopy was performed on a Jeol JEM-1230 instrument (Jeol Ltd., Tokyo, Japan) at the Molecular Imaging Centre (University of Bergen). Pictures were acquired using the GATAN multiscan camera (Gatan Inc, Pleasanton, CA, USA).

2.4. Mitochondrial respiration

Oxygen consumption rates were analysed using Oxygraph O2K and DatLab software (Oroboros Instruments, Austria). The oxygen consumption rates were normalized to the number of cells in each chamber. Measurements in intact hepatocytes were performed in RPMI 1640 cell culture medium (without FBS) after sequential additions of oligomycin (1.8µg/ml), carbonylcyanide- 4-(trifluoromethoxy)-phenylhydrazone (FCCP) (titrated to maximal activity, titration range 0.1– 0.27 mM), rotenone (0.5 µM), antimycin A (2.5 µM). The respiration medium for permeabilised cells was 0.5 mM EGTA, 3 mM $MgCl_2 \cdot 6H_2O$, 60 mM K-lactobionate, 20 mM taurine, 10 mM KH_2PO_4, 20 mM HEPES, 110 mM sucrose and

1 g/l bovine serum albumin. The additional supplements were malate (1.8 mM), glutamate (9.1 mM), succinate (9.1 mM), digitonin (3.7 µM) and ADP (2.3 mM).

2.5. Citrate synthase measurements

Citrate synthase activity was measured in $2x10^5$ cells/ml in incubation medium as previously described [24].

2.6. Flow cytometry

Viable cells were analysed only for their FSC-H and SSC-H properties in a BD FACSCalibur flow cytometer (BD Biosciences, San Jose, CA, USA). For protein analysis, hepatocytes were fixed (3.7% para-formaldehyde in PBS), permeabilised (methanol) and immunostained according to the protocol provided by Cell Signaling Technology Inc. Following labelling with Alexa Fluor 488-conjugated secondary antibody (Invitrogen, Carlsbad, CA, USA), the analysis was performed using an Accuri C6 flow cytometer (Accuri Cytometers Inc., Ann Arbor, MI, USA)

2.7. *RNA isolation and quantitative real-time PCR*

RNA was extracted from tissue samples using RNAeasy Mini kit (Qiagen, Hilden, Germany). Reverse transcription was performed using High-Capacity Reverse Transcription Kit (Applied Biosystems, Foster City, CA, USA). Quantitative PCR was performed in the LightCycler 480 detection system using the LightCycler 480 Probes master kit (Roche, Basel, Switzerland). The following genes were analysed using specific FAM probes and primers from Applied Biosystems: Cytochrome *c* oxidase (COX), *Cox4i1*,Rn00665001_g1; Cytochrome *c* somatic (Cyt *c*), Rn00820639_g1; Transcriptional Factor A mitochondrial (TFAM), Rn_00580051_m1; Carnitine palmitoyl transporter 1 (CPT-1), Rn0050702_m1; CPT-2,

Rn00563995_m1; Rn01495769_m1: Carnitine/acylcarnitine translocase (CACT) (Slc25a20), Rn00588652; Acyl-CoA oxidase-1 (ACOX-1) , Rn00569216; 3-hydroxy-3-methylglutaryl-CoA synthase 2 (mitochondrial) (HMGCS-2), Rn00597339: Nuclear respiratory factor 1 (NRF-1) Rn01455958_m1; Uncoupling protein 3 (UCP3), Rn00565874_m1. For reference we used the 18s rRNA control kit FAM-TAMRA (RT-CKFT-18s) from Eurogentec (Liége, Belgium).

2.8. Mitochondrial DNA quantification

DNA was isolated from primary hepatocytes using DNA Blood and Tissue Kit (Qiagen). Specific primer for mitochondrial DNA (mtDNA), ND1 (Rn03296764_s1), was purchased from Applied Biosystems and nuclear DNA (nDNA) primer 18S (RT-CKFT-18s) from Eurogentec. Real-time PCR was carried out on Lightcycler 480 detection system (Roche) and the mtDNA/nDNA ratio was calculated [25].

2.9. Western Blots

Protein concentrations were measured using the Thermo Scientific Pierce BCA Protein Assay Kit (Thermo Scientific Pierce Protein Biology, Rockford, IL, USA). SDS-PAGE and Western blotting were performed using the Invitrogen system, with PVDF membranes. Detection was done using secondary antibody conjugated to HRP from BioRad Laboratories Inc (Hercules, CA, USA) and ECL Western Blotting Substrate (Thermo Scientific Pierce Protein Biology) in a LAS-3000 imaging system (Fujifilm, Tokyo, Japan). Pixel analysis was performed using Multi Gauge V2.2. software (Fujifilm).

2.10. Statistical Analysis

Three independent experiments were performed. Data were analysed using a two sided t-test, and a p-value <0.05 was considered to indicate statistical significance.

3. Results

3.1. Mitochondrial biogenesis coincides with hypertrophy in hepatocytes of TTA-treated rats

The hypolipidemic effect of TTA was first confirmed by measuring levels of cholesterol, triglycerides and phospholipids in blood plasma, after treating the rats for 3 weeks (data not shown). The TTA-treated rats had significantly larger livers (Fig. 1A), which also was in accordance with previous studies [26]. Hepatocytes were isolated from these livers in order to characterize in more detail the effects of TTA on cellular phenotype and mitochondrial biomass. We found that the hepatocyte protein content tended to increase, although the relatively large standard deviation prevented statistical significance. This was, however, accompanied by higher levels of the mitochondrial biomarkers mtDNA and citrate synthase, of which the latter demonstrated a statistically significant change (Fig 1A). Furthermore, flow cytometry analysis showed that cells from TTA-treated rats were larger (forward scatter, FSC-H), and the cellular granularity was increased (side scatter, SSC-H) (Fig. 1B).

The cellular morphology was investigated in more detail by transmission electron microscopy (Fig. 1C). In accordance with the data above (Fig 1B), hepatocytes from TTA-treated rats were observed to be larger in size, and have a richer granular content compared to the control cells. Apparently, this included increased number of mitochondria and peroxisomes, as well as glycogen particles indicating alterations in carbohydrate metabolism. There were also significant changes in the morphology of rough and smooth endoplasmatic reticulum. Observations in isolated hepatocytes correlated with intact liver tissue.

In order to confirm that TTA induced mitochondrial biogenesis, we measured mRNA expression of several associated markers, as well as proteins involved in fatty acid metabolism, in samples from liver. The data demonstrated a moderate increase in two key proteins in mitochondrial biogenesis, NRF-1 and TFAM, as well as mRNA levels of two proteins of the respiratory system, COX and Cyt *c* (Fig. 1D). Moreover, increased mRNA expression of CPT-1, CPT-2, CACT and HMGSC-1 indicated upregulation of mitochondrial fatty acid oxidation and ketogenesis. This was also associated with a significant increase in UCP3 expression, confirming previous results [27]. The upregulation of these factors, as well as ACOX-1, supports PPARα activation. These data confirm that TTA induces expression of multiple genes involved in mitochondrial biogenesis and function.

3.2. Stimulated mitochondrial respiration in hepatocytes from TTA-treated rats

In order to determine if the observed increase in mitochondrial biogenesis influenced mitochondrial respiratory function, we measured oxygen consumption rates. The data demonstrated that the respiratory rate in RPMI cell culture medium (ROUTINE) was increased 2.6 fold in hepatocytes of TTA-treated rats (Fig. 2A). This change was accompanied by increased non-phosphorylating respiration (LEAK), when ATP synthase was inhibited with oligomycin. Furthermore, the capacity of the electron transport system (ETS) was increased 2.5 fold, measured after full uncoupling with FCCP. Interestingly, in contrast to control hepatocytes, a significant fraction of the respiration in intact hepatocytes from TTA-treated rats were independent of respiratory complex I, as observed after addition of the complex I inhibitor rotenone (ETSrot). These data further reveal that both TTA and control cells utilized about 50% of the maximum capacity (ETS) under normal cell culture conditions (ROUTINE). However, the larger fraction of LEAK respiration in TTA-treated rats, suggests that more of the respiratory activity is uncoupled from ATP synthesis.

In order to study the modulation of oxidative phosphorylation in more detail, we permeabilised the cells to allow free flux of substrates into the mitochondria (Fig. 2B). Consistent with the findings in intact cells, respiration in presence of malate, glutamate and succinate (MGS) was significantly increased after treatment with TTA. Addition of ADP demonstrated that there was an increase in the oxidative phosphorylation capacity (OXPHOS). Both the LEAK and ETS respiratory rates were higher, confirming the results in intact cells (Fig 2A). However, addition of rotenone had minor effect in both cell types. The phosphorylation system control ratio (OXPHOS/ETS) was calculated to 0.45±0.06 and 0.81±0.18 in control and TTA-treated cells, respectively, suggesting that the limitation of electron flux exerted by the phosphorylation system was reduced.

3.3. TTA-treatment activates mTOR signalling in rat liver

The hypertrophic response in hepatocytes of TTA-treated rats was found to be accompanied by an increase in mitochondrial biomass and oxidative capacity. We further examined if these effects were associated with regulation of Akt, ERK1/2 and mTOR, three key signalling factors of cell homeostasis and adaptation. Flow cytometry analysis indicated that expression of mTOR was increased (Fig. 3A), and activation of this pathway was supported by increased phosphorylation of the downstream actors 4E-BP1 and eIF4G, as demonstrated by western blotting (Fig. 3B). The protein levels of these factors were also increased. The level of Akt was unchanged or slightly reduced, but we observed a minor increase in phosphorylation at Ser473 (Fig. 3A). Finally, we found that the protein level and phosphorylation of ERK1/2 was increased in TTA treated rats; although statistics could not be calculated since we only had samples from two rats in each group for this analysis (Fig. 3B).

4. Discussion

This work demonstrates that the significant increase in mitochondrial oxidation capacity observed in rat hepatocytes after treatment with TTA can be explained by induction of mitochondrial biogenesis accompanied by increased mitochondrial respiration. The adaptive mechanism involved PPAR-activation in addition to signalling via ERK1/2 and mTOR, and was associated with cellular hypertrophy.

Previous studies have demonstrated that the modified fatty acid TTA act as a pan-PPAR activator and regulate processes of lipid and energy metabolism in animals [17,18,19,20] . Activation of PPARα was confirmed by upregulated mRNA expression of ACOX, CPT II and UCP3, representing target genes of this transcription factor [27,28]. Furthermore, our study showed that the increased liver weight involved cellular organelle amplifications, a known stress response after increased functional load in the liver [29]. The increase in hepatocyte cell size, granularity and protein content was consistent with cellular hypertrophy. Hypertrophy is a well-known effect of PPARα activation that seems restricted to rodents and not humans [30]. Induction of mitochondrial biogenesis was confirmed by measuring mtDNA, citrate synthase activity and mRNA expression of mitochondrial proteins. Although the morphology appeared less organized in samples from TTA-treated rats, there were no signs of cellular toxicity and the biochemical function was intact. Previous data from long term rat experiments (50 weeks) [27] and clinical studies [31] have shown that TTA is well tolerated.

This study suggest that mTOR, possibly via interaction with ERK1/2 and Akt, may be involved in an adaptive stress response leading to hypertrophy and mitochondrial biogenesis in hepatocytes after treatment with TTA. This may share similarity with the adaptive signalling response of mitochondrial biogenesis observed in muscle after exercise [32]. Furthermore, TTA has effects in common fasting condition, including increased fatty acid

oxidation and ketogenesis, which have been associated with PGC1α [33], another player in the mTOR network [34]. Moreover, recently mTORC1 was shown to act together with PPARα in the regulation of fasting-induced ketogenesis [7], whereas in adipocytes, PPARγ interacts with mTOR to regulate hypertrophy [35]. These findings suggest that the observed effects of TTA might involve crosstalk between PPARs and mTOR.

Mitochondrial respiration was significantly increased together with induction of mitochondrial biogenesis in rat hepatocytes after treatment with TTA. This included increased capacities of the ETS as well as OXPHOS. However, whereas ADP-induced respiration closely balanced the ETS capacity in hepatocytes from TTA-treated rats, the ETS capacity exceeded the ADP-induced respiration in control hepatocytes. This suggests that the capacity to phosphorylate ADP to ATP is selectively strengthened in TTA-treated hepatocytes. Furthermore, the uncoupled respiration (LEAK) was increased after the treatment, supporting previous studies of fatty acid-driven respiration [20]. Whether or not this is associated with the significant up-regulation of UCP3 remains unclear since the role of this protein is still unknown. However, potential functions are related to metabolic balancing [36] as well as handling of reactive oxygen species (ROS) [37]. We also observed a significantly increased fraction of rotenone-insensitive respiration. This may be associated with the high rates of fatty acid β-oxidation, feeding electrons into the ubiquinone pool via the ETFP-ubiquinone oxidoreductase [38], thereby bypassing the rotenone sensitive complex I.

In summary, these results suggest that the increased mitochondrial biogenesis and respiration in rat hepatocytes after treatment with TTA involves coordinated regulation of oxidative metabolism via PPARs in association with a hypertrophic response possibly mediated via mTOR. How these pathways may interact under these conditions is yet to be determined. Our results also highlight the extensive adaptability of hepatic mitochondria under metabolically demanding conditions.

Acknowlegdements

We thank Nina Lied Larsen, Kari Williams and Ingrid Strand for superior technical assistance. We are also grateful to Prof Stein Ove Døskeland for valuable discussions related to this study. This research was supported by the Meltzer Foundation (University of Bergen) and the Norwegian Research Council.

References

[1] E. Sahin, R.A. DePinho, Axis of ageing: telomeres, p53 and mitochondria, Nat Rev Mol Cell Biol 13 (2012) 397-404.

[2] R.J. DeBerardinis, J.J. Lum, G. Hatzivassiliou, C.B. Thompson, The biology of cancer: metabolic reprogramming fuels cell growth and proliferation, Cell metabolism 7 (2008) 11-20.

[3] I.V. Murray, J.F. Proza, F. Sohrabji, J.M. Lawler, Vascular and metabolic dysfunction in Alzheimer's disease: a review, Experimental biology and medicine 236 (2011) 772-782.

[4] A.A. Bremer, M. Mietus-Snyder, R.H. Lustig, Toward a unifying hypothesis of metabolic syndrome, Pediatrics 129 (2012) 557-570.

[5] Z. Ament, M. Masoodi, J.L. Griffin, Applications of metabolomics for understanding the action of peroxisome proliferator-activated receptors (PPARs) in diabetes, obesity and cancer, Genome Med 4 (2012) 32.

[6] W. Wahli, L. Michalik, PPARs at the crossroads of lipid signaling and inflammation, Trends Endocrinol Metab 23 (2012) 351-363.

[7] S. Sengupta, T.R. Peterson, M. Laplante, S. Oh, D.M. Sabatini, mTORC1 controls fasting-induced ketogenesis and its modulation by ageing, Nature 468 (2010) 1100-1104.

[8] J.J. Howell, B.D. Manning, mTOR couples cellular nutrient sensing to organismal metabolic homeostasis, Trends in endocrinology and metabolism: TEM 22 (2011) 94-102.

[9] M. Moreno, A. Lombardi, E. Silvestri, R. Senese, F. Cioffi, F. Goglia, A. Lanni, P. de Lange, PPARs: Nuclear Receptors Controlled by, and Controlling, Nutrient Handling through Nuclear and Cytosolic Signaling, PPAR Res 2010 (2010).

[10] H. Zhou, S. Huang, The complexes of mammalian target of rapamycin, Curr Protein Pept Sci 11 (2010) 409-424.

[11] M. Wan, Karla F. Leavens, D. Saleh, Rachael M. Easton, David A. Guertin, Timothy R. Peterson, Klaus H. Kaestner, David M. Sabatini, Morris J. Birnbaum, Postprandial Hepatic Lipid Metabolism Requires Signaling through Akt2 Independent of the Transcription Factors FoxA2, FoxO1, and SREBP1c, Cell Metabolism 14 (2011) 516-527.

[12] J.R. Speakman, S.E. Mitchell, Caloric restriction, Molecular aspects of medicine 32 (2011) 159-221.

[13] F. Bost, The extracellular signal-regulated kinase isoform ERK1 is specifically required for in vitro and in vivo adipogenesis, Diabetes 54 (2005) 402-411.

[14] F.W. Booth, D.B. Thomason, Molecular and cellular adaptation of muscle in response to exercise: perspectives of various models, Physiol Rev 71 (1991) 541-585.

[15] Z. Yao, A.W. Jones, E. Fassone, M.G. Sweeney, M. Lebiedzinska, J.M. Suski, M.R. Wieckowski, N. Tajeddine, I.P. Hargreaves, T. Yasukawa, G. Tufo, C. Brenner, G. Kroemer, S. Rahman, G. Szabadkai, PGC-1beta mediates adaptive chemoresistance associated with mitochondrial DNA mutations, Oncogene (2012).

[16] R.M. Reznick, G.I. Shulman, The role of AMP-activated protein kinase in mitochondrial biogenesis, J Physiol 574 (2006) 33-39.

[17] R.K. Berge, K.J. Tronstad, K. Berge, T.H. Rost, H. Wergedahl, O.A. Gudbrandsen, J. Skorve, The metabolic syndrome and the hepatic fatty acid drainage hypothesis, Biochimie 87 (2005) 15-20.

[18] R.K. Berge, J. Skorve, K.J. Tronstad, K. Berge, O.A. Gudbrandsen, H. Grav, Metabolic effects of thia fatty acids, Curr Opin Lipidol 13 (2002) 295-304.

[19] L. Madsen, M. Guerre-Millo, E.N. Flindt, K. Berge, K.J. Tronstad, E. Bergene, E. Sebokova, A.C. Rustan, J. Jensen, S. Mandrup, K. Kristiansen, I. Klimes, B. Staels, R.K. Berge, Tetradecylthioacetic acid prevents high fat diet induced adiposity and insulin resistance, J Lipid Res 43 (2002) 742-750.

[20] H.J. Grav, K.J. Tronstad, O.A. Gudbrandsen, K. Berge, K.E. Fladmark, T.C. Martinsen, H. Waldum, H. Wergedahl, R.K. Berge, Changed energy state and increased mitochondrial beta-oxidation rate in liver of rats associated with lowered proton electrochemical potential and stimulated uncoupling protein 2 (UCP-2) expression: evidence for peroxisome proliferator-activated receptor-alpha independent induction of UCP-2 expression, J Biol Chem 278 (2003) 30525-30533.

[21] L. Madsen, L. Froyland, H.J. Grav, R.K. Berge, Up-regulated delta 9-desaturase gene expression by hypolipidemic peroxisome-proliferating fatty acids results in increased oleic acid content in liver and VLDL: accumulation of a delta 9-desaturated metabolite of tetradecylthioacetic acid, J Lipid Res 38 (1997) 554-563.

[22] K.E. Fladmark, O.T. Brustugun, G. Mellgren, C. Krakstad, R. Boe, O.K. Vintermyr, H. Schulman, S.O. Doskeland, Ca2+/calmodulin-dependent protein kinase II is required for microcystin-induced apoptosis, J Biol Chem 277 (2002) 2804-2811.

[23] G. Mellgren, O.K. Vintermyr, S.O. Doskeland, Okadaic acid, cAMP, and selected nutrients inhibit hepatocyte proliferation at different stages in G1: modulation of the cAMP effect by phosphatase inhibitors and nutrients, J Cell Physiol 163 (1995) 232-240.

[24] S. Stadlmann, K. Renner, J. Pollheimer, P.L. Moser, A.G. Zeimet, F.A. Offner, E. Gnaiger, Preserved coupling of oxidative phosphorylation but decreased mitochondrial

respiratory capacity in IL-1beta-treated human peritoneal mesothelial cells, Cell biochemistry and biophysics 44 (2006) 179-186.

[25] L. He, P.F. Chinnery, S.E. Durham, E.L. Blakely, T.M. Wardell, G.M. Borthwick, R.W. Taylor, D.M. Turnbull, Detection and quantification of mitochondrial DNA deletions in individual cells by real-time PCR, Nucleic Acids Res 30 (2002) e68.

[26] h. Kryvi, A. Aarsland, R.K. Berge, Morphologic effects of sulfur-substituted fatty acids on rat hepatocytes with special reference to proliferation of peroxisomes and mitochondria, Journal of Structural Biology 103 (1990) 257-265.

[27] N.F. Vigerust, D. Cacabelos, L. Burri, K. Berge, H. Wergedahl, B. Christensen, M. Portero-Otin, A. Viste, R. Pamplona, R.K. Berge, B. Bjørndal, Fish oil and 3-thia fatty acid have additive effects on lipid metabolism but antagonistic effects on oxidative damage when fed to rats for 50 weeks, The Journal of Nutritional Biochemistry.

[28] K. Berge, K.J. Tronstad, E.N. Flindt, T.H. Rasmussen, L. Madsen, K. Kristiansen, R.K. Berge, Tetradecylthioacetic acid inhibits growth of rat glioma cells ex vivo and in vivo via PPAR-dependent and PPAR-independent pathways, Carcinogenesis 22 (2001) 1747-1755.

[29] R. Schulte-Hermann, Induction of liver growth by xenobiotic compounds and other stimuli, CRC critical reviews in toxicology 3 (1974) 97-158.

[30] L. Burri, G.H. Thoresen, R.K. Berge, The Role of PPARalpha Activation in Liver and Muscle, PPAR Res 2010 (2010).

[31] R.J. Pettersen, M. Salem, J. Skorve, R.J. Ulvik, R.K. Berge, J.E. Nordrehaug, Pharmacology and safety of tetradecylthioacetic acid (TTA): phase-1 study, Journal of cardiovascular pharmacology 51 (2008) 410-417.

[32] L. Wang, H. Mascher, N. Psilander, E. Blomstrand, K. Sahlin, Resistance exercise enhances the molecular signaling of mitochondrial biogenesis induced by endurance exercise in human skeletal muscle, J Appl Physiol 111 (2011) 1335-1344.

[33] C. Handschin, B.M. Spiegelman, Peroxisome proliferator-activated receptor gamma coactivator 1 coactivators, energy homeostasis, and metabolism, Endocrine reviews 27 (2006) 728-735.

[34] J.T. Cunningham, J.T. Rodgers, D.H. Arlow, F. Vazquez, V.K. Mootha, P. Puigserver, mTOR controls mitochondrial oxidative function through a YY1-PGC-1[agr] transcriptional complex, Nature 450 (2007) 736-740.

[35] K.V. Guntur, A. Guilherme, L. Xue, A. Chawla, M.P. Czech, Map4k4 negatively regulates peroxisome proliferator-activated receptor (PPAR) gamma protein translation by suppressing the mammalian target of rapamycin (mTOR) signaling pathway in cultured adipocytes, The Journal of biological chemistry 285 (2010) 6595-6603.

[36] D. Ricquier, Respiration uncoupling and metabolism in the control of energy expenditure, The Proceedings of the Nutrition Society 64 (2005) 47-52.

[37] R.J. Mailloux, M.E. Harper, Uncoupling proteins and the control of mitochondrial reactive oxygen species production, Free radical biology & medicine 51 (2011) 1106-1115.

[38] F.E. Frerman, Reaction of electron-transfer flavoprotein ubiquinone oxidoreductase with the mitochondrial respiratory chain, Biochimica et biophysica acta 893 (1987) 161-169.

Legends

Fig. 1. Hypertrophy and mitochondrial biogenesis in hepatocytes of TTA-treated rats. (A) Rat livers were weighed directly after resection. Hepatocytes were isolated from parallel animals. Protein content and citrate synthase activity was determined in isolated hepatocytes, and normalized to cell number. The amount of mtDNA was measured relative to nDNA in liver tissue. Fold change was calculated relative to the corresponding control. The data are presented as mean ± S.D. of three rats, with each measurement performed in duplicate or triplicate. (B) Isolated hepatocytes were analysed by flow cytometry, and viable cells were gated from a population of 10000 cells. The histograms show representative data from forward and side scatter (FSC-H and SSC-H, respectively; A.U., arbitrary units). The data are derived from >10 measurements in both groups, in two independent experiments. (C) Transmission electron microscopy of isolated primary hepatocytes (left hand panel) and liver tissue (right hand panel). The samples were either from control (upper row) or TTA-treated (lower row) rats. The images are a representative selection of >20 pictures of different sections from two separate experiments. Indicated structures: Bile caniliculi in tissue, BC; glycogen, Gly; mitochondria, Mt; Mt-ph, mitophagy; peroxisomes, P; Rough endoplasmatic reticulum ,RER; smooth endoplasmatic reticulum, SER. (D) mRNA expression of selected genes in rat liver. The data represent mean ± S.D. of three rats, with each measurement performed in triplicate. The genes are classified based on function.
*$p<0.05$ compared to control.

Fig. 2. TTA treatment induced respiration in rat hepatocytes. Mitochondrial respiration was measured in hepatocytes (45- 90*10^5 cells/ml) isolated from control and TTA-treated rats. Oxygen consumption rates were determined after sequential additions of modulators. (A) Basal respiration (ROUTINE) in intact cells was measured in RPMI 1640 medium. Addition

of oligomycin (LEAK) was followed by titration with the uncoupler FCCP to give electron transport system capacity (ETS). Rotenone was then added (ETSrot), and finally antimycin A to give the background activity. The figure shows mean ± S.D. of two experiments with duplicate measurements. (B) Cells were permeabilised with digitonin in respiration medium. The basal respiratory rate was determined in the presence of malate, glutamate and succinate as substrates (MGS). ADP was then added to determine the oxidative phosphorylation capacity (OXPHOS). LEAK, ETS, ETSrot and background were then determined as described above. The figure shows representative data from one of three independent experiments, and the results are presented as mean ± S.D. of four measurements

*$p<0.05$ compared to control.

Fig. 3. Effects on Akt/ERK/mTOR signaling. (A) Immunodetection by flow cytometry was performed to analyse the protein expression and phosphorylation status of Akt and mTOR. The figure shows representative histograms, and the column diagram display fold change in geometric mean after TTA-treatment. Data are presented as mean ± S.D, and represents two experiments with triplicate measurements. (B) Western blot analysis was performed to detect protein expression and phosphorylation. The figure shows representative blots from three independent experiments with cells from three different animals. The band intensities were quantified and normalised to β-actin, before calculating fold change relative to control (mean ± S.D., n=2-3).

*$p<0.05$ comparing TTA treated samples with untreated ones.

Figure 1

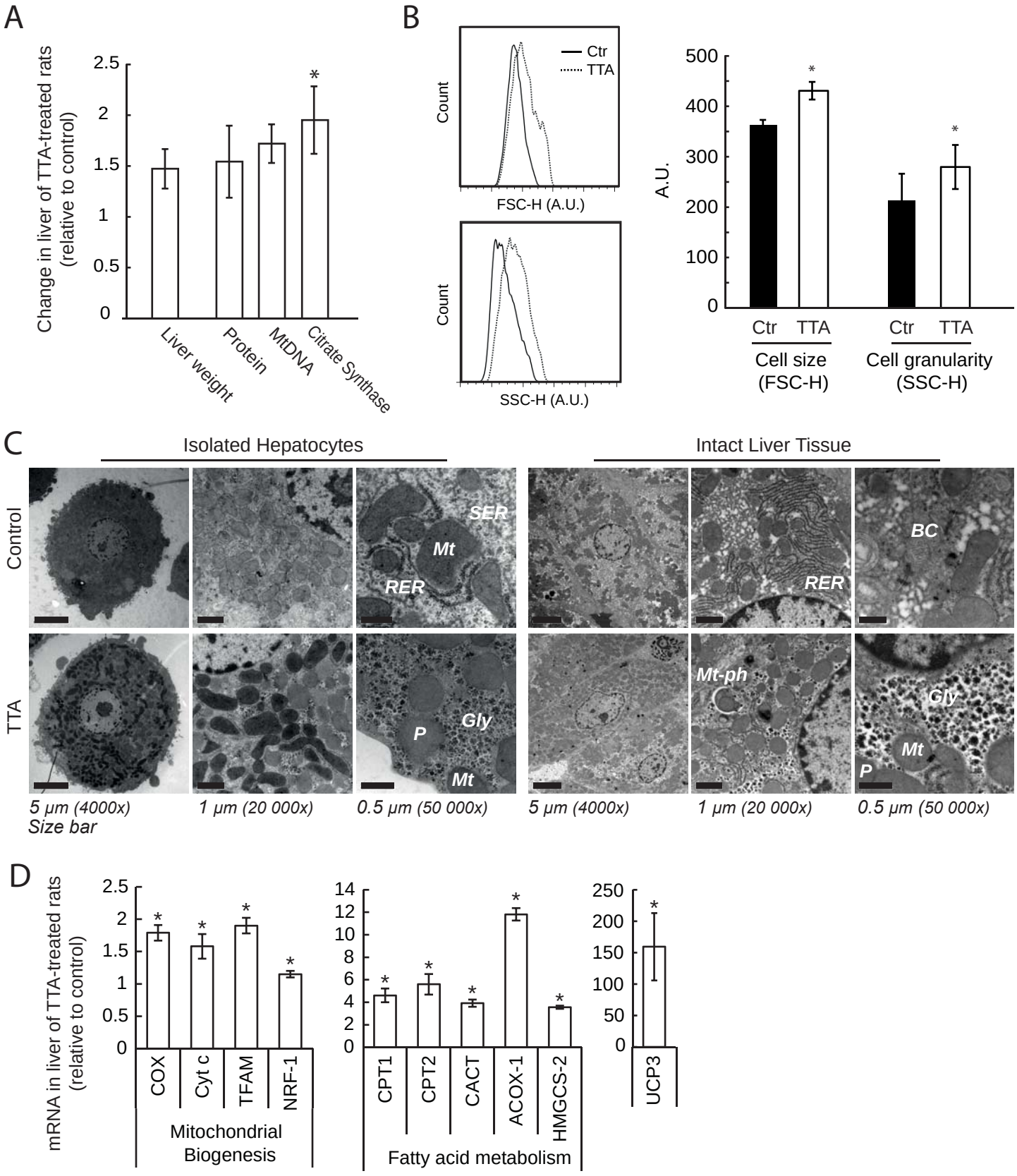
A
Change in liver of TTA-treated rats (relative to control)
2.5
2
1.5
1
0.5
0
*
Liver weight
Protein
MtDNA
Citrate Synthase
B
Count
Ctr
TTA
FSC-H (A.U.)
SSC-H (A.U.)
A.U.
500
400
300
200
100
0
Ctr
TTA
Cell size (FSC-H)
Cell granularity (SSC-H)
C
Isolated Hepatocytes
Intact Liver Tissue
Control
TTA
SER
Mt
RER
BC
Mt-ph
Gly
P
5 µm (4000x)
1 µm (20 000x)
0.5 µm (50 000x)
Size bar
D
mRNA in liver of TTA-treated rats (relative to control)
COX
Cyt c
TFAM
NRF-1
Mitochondrial Biogenesis
CPT1
CPT2
CACT
ACOX-1
HMGCS-2
Fatty acid metabolism
UCP3

Figure 2

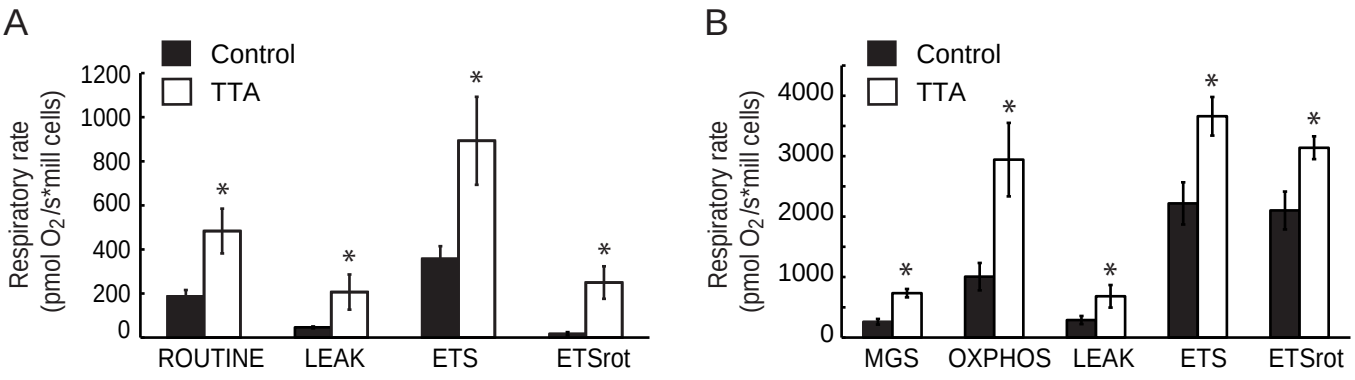
A
Control
TTA
Respiratory rate
(pmol O2/s*mill cells)
1200
1000
800
600
400
200
0
ROUTINE
LEAK
ETS
ETSrot
B
Control
TTA
Respiratory rate
(pmol O2/s*mill cells)
4000
3000
2000
1000
0
MGS
OXPHOS
LEAK
ETS
ETSrot

Figure 3

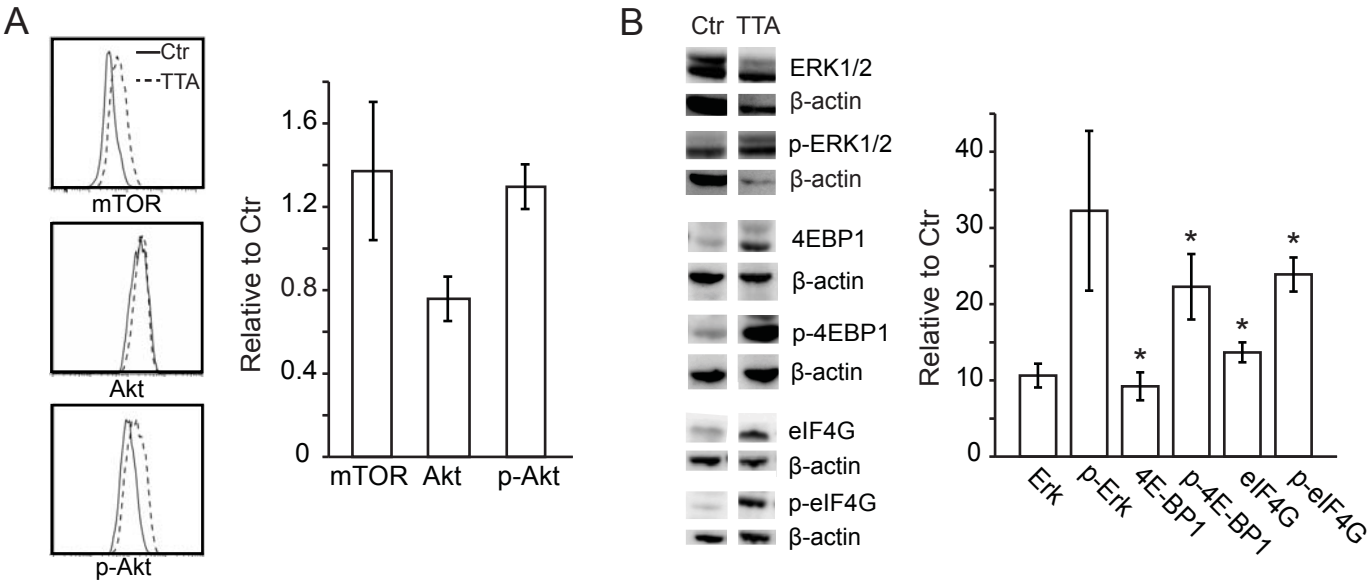
A
Ctr
TTA
mTOR
Akt
p-Akt
Relative to Ctr
1.6
1.2
0.8
0.4
0
mTOR
Akt
p-Akt
B
Ctr
TTA
ERK1/2
β-actin
p-ERK1/2
β-actin
4EBP1
β-actin
p-4EBP1
β-actin
eIF4G
β-actin
p-eIF4G
β-actin
Relative to Ctr
40
30
20
10
0
Erk
p-Erk
4E-BP1
p-4E-BP1
eIF4G
p-eIF4G
*